

**Strain effects on the spin polarized electron gas in  $ABO_3/SrTiO_3$  (A=Pr, Nd and B=Al, Ga) heterostructures**

S. Nazir and U. Schwingenschlögl

Citation: *Applied Physics Letters* **102**, 141604 (2013); doi: 10.1063/1.4801514

View online: <http://dx.doi.org/10.1063/1.4801514>

View Table of Contents: <http://scitation.aip.org/content/aip/journal/apl/102/14?ver=pdfcov>

Published by the *AIP Publishing*

---

The advertisement features a blue background with a photograph of the Model PS-100 probe station. The text is arranged as follows: 'NEW' in orange, 'Model PS-100' in large blue font, 'Preconfigured Tabletop Probe Station' in smaller blue font, the Lake Shore CRYOTRONICS logo (a blue square with a white diagonal line) and 'Lake Shore CRYOTRONICS' in white, and the tagline 'An affordable solution for a wide range of research' in white italicized font.

**NEW**  
**Model PS-100**  
Preconfigured Tabletop  
Probe Station

 **Lake Shore**  
CRYOTRONICS

*An affordable solution for  
a wide range of research*

## Strain effects on the spin polarized electron gas in $ABO_3/SrTiO_3$ (A = Pr, Nd and B = Al, Ga) heterostructures

S. Nazir and U. Schwingenschlög<sup>a)</sup>

Physical Science & Engineering Division, KAUST, Thuwal 23955-6900, Kingdom of Saudi Arabia

(Received 13 November 2012; accepted 27 March 2013; published online 11 April 2013)

The spin polarized two dimensional electron gas in the correlated  $ABO_3/SrTiO_3$  (A = Pr, Nd and B = Al, Ga) heterostructures is investigated by *ab-initio* calculations using density functional theory. Structural relaxation shows a strong buckling at and near the  $TiO_2$  terminated *n*-type interface (IFs) due to significant  $TiO_6$  octahedral distortions. We find in all cases, metallic states in a very narrow region of the  $SrTiO_3$ , in agreement with experimental results. We demonstrate that the interface magnetism strongly reacts to the magnitude of the lattice strain. The orbital occupations and, hence, the charge carrier density change systematically as a function of the lattice mismatch between the component materials. © 2013 AIP Publishing LLC.

[<http://dx.doi.org/10.1063/1.4801514>]

Perovskite oxide interfaces (IFs) exhibit controllable electronic properties that are of interest for magnetic oxide devices.<sup>1–3</sup> For example, the two dimensional electron gas (2DEG) formed in the  $LaAlO_3/SrTiO_3$  heterostructure has emerged as a subject of intensive experimental and theoretical research due to both potential nanoscale device applications and interest in fundamental physics.<sup>4–7</sup> For example, coexistence of superconductivity and ferromagnetism has been observed, while usually ferromagnetism counteracts the electron pairing and hence is incompatible with superconductivity.<sup>8,9</sup> Only very recently experiments have shown that the electronic reconstruction at the  $LaAlO_3/SrTiO_3$  IF is not enough to induce ferromagnetism but that a critical  $LaAlO_3$  thickness is required, similar to the formation of metallicity.<sup>10</sup> The authors suggest that IF disorder and local strain play an important role. The effect of strain on the electronic properties has been studied by epitaxial growth of  $LaAlO_3/SrTiO_3$  heterostructures on different substrates, and it has been demonstrated that tensile strain destroys the 2DEG, while compressive strain retains it.<sup>11</sup> A metallic IF and superconductivity are also found for the closely related  $LaGaO_3/SrTiO_3$  heterostructure.<sup>12–15</sup> Moreover, a high charge carrier density combined with a substantial mobility have been reported for the correlated  $LaTiO_3/SrTiO_3$  heterostructure.<sup>16–20</sup>

Very recently, spin polarized 2DEGs have been observed in epitaxial  $ABO_3/SrTiO_3$  (A = Pr, Nd and B = Al, Ga) heterostructures, which are comparable to  $LaAlO_3/SrTiO_3$  in terms of the charge carrier density and mobility.<sup>21,22</sup> These papers argue that the combined effect of electronic correlations and large octahedral distortions due to IF strain control the charge carrier density and mobility of the 2DEG. A large lattice mismatch between the component materials limits the mobility. For  $NdGaO_3/SrTiO_3$ , therefore a higher mobility would be expected than for  $LaAlO_3/SrTiO_3$  as the lattice mismatch between  $NdAlO_3$  and  $SrTiO_3$  is smaller. However, the mobilities of the two systems turn out to be similar because of impurity scattering.<sup>21</sup>

Furthermore, it is found that the injected electrons from the IF  $NdO$  and  $PrO$  layers mostly go to the Ti atoms in the IF  $TiO_2$  layer. Charge confinement occurs within a few  $SrTiO_3$  unit cells away from the IF, whereas the cation intermixing is limited to one or two unit cells. Because of the complicated interplay of different effects in the experiment, the detailed dependence of the IF states on intrinsic properties such as lattice mismatch and buckling could not be thoroughly determined. However, exact knowledge about the thickness of the correlated 2DEG and understanding of the governing factors are essential in order to maximize device performance.

In this context, we present a theoretical study of the electronic and magnetic properties of the  $TiO_2$  terminated *n*-type IFs in the  $ABO_3/SrTiO_3$  (A = Pr, Nd and B = Al, Ga) heterostructures. After describing the computational details and giving some remarks on the parent compounds  $ABO_3$  and  $SrTiO_3$ , we will turn to the  $ABO_3/SrTiO_3$  heterostructures to study the effects of structural relaxation and discuss the IF states. We determine quantitatively how the lattice mismatch between the component materials influences the orbital occupation, charge carrier density, and spin polarization.

All calculations employ the full-potential linearized augmented plane-wave method in the framework of density functional theory, using the WIEN2K code.<sup>23</sup> The spin polarized generalized gradient approximation plus onsite Coulomb interaction approach (GGA+*U*) is applied for the exchange-correlation potential with  $U = 4$  eV for the Ti *3d* orbitals and  $U = 7.5$  eV for the Nd and Pr *4f* orbitals. The spin-orbit coupling (SOC) is also taken into account. For the wave function expansion inside the atomic spheres, a maximum value of  $\ell_{max} = 12$  is chosen and the plane-wave cutoff is set to  $R_{mt}K_{max} = 6$  with  $G_{max} = 24$ . The muffin-tin sphere radius  $R_{mt}$  (in atomic units) is chosen as 2.00 for Sr, 1.90 for Ti, 2.50 for Pr and Nd, 1.75 for Al, 1.80 for Ga, and 1.62 for O. Moreover, a  $11 \times 11 \times 1$  mesh with 21 points within the irreducible wedge of the Brillouin zone is found to be well converged. Self-consistency is assumed for a total energy convergence of less than  $10^{-3}$  Ry.

<sup>a)</sup>udo.schwingenschlogl@kaust.edu.sa. Tel.: +966(0)544700080

SrTiO<sub>3</sub> has a band gap of 3.2 eV and crystallizes in a cubic structure with an experimental lattice constant of 3.905 Å.<sup>4</sup> Its electronic structure has been subject of various studies, see Ref. 24, for example. NdGaO<sub>3</sub>, NdAlO<sub>3</sub>, and PrAlO<sub>3</sub> have pseudocubic structures with experimental lattice constants of 3.860 Å, 3.784 Å, and 3.762 Å, respectively.<sup>25,26</sup> The spin polarized total densities of states (DOSs) obtained using these lattice constants are shown in Fig. 1 for GGA+*U* (top row) and GGA+*U*+SOC (bottom row) calculations. The figure shows sharp Pr and Nd 4*f* peaks at the Fermi energy (*E<sub>F</sub>*) for the GGA+*U* approach, whereas the GGA+*U*+SOC approach results in a large band gap of 3.2 eV for NdGaO<sub>3</sub> in agreement with the experiment, see also Ref. 27. Similarly, band gaps of 3.9 eV and 3.6 eV are found for PrAlO<sub>3</sub> and NdAlO<sub>3</sub>. Bulk SrTiO<sub>3</sub> exhibits a 2.7 eV band gap both in the GGA+*U* and GGA+*U*+SOC schemes. We obtain for the GGA+*U*+SOC approach magnetic moments of 2.99 μ<sub>B</sub> and 2.98 μ<sub>B</sub> for the Nd atoms in NdGaO<sub>3</sub> and NdAlO<sub>3</sub>, respectively, and a Pr magnetic moment of 1.98 μ<sub>B</sub> in PrAlO<sub>3</sub>.

The NdGaO<sub>3</sub>/SrTiO<sub>3</sub>, PrAlO<sub>3</sub>/SrTiO<sub>3</sub>, and NdAlO<sub>3</sub>/SrTiO<sub>3</sub> heterostructures are modeled by means of supercells with averaged lattice constants of 3.881 Å, 3.845 Å, and 3.834 Å in the *ab*-plane, respectively, for lattice matching. Each supercell consists of 4 unit cells of ABO<sub>3</sub> and 10 unit cells of SrTiO<sub>3</sub> (~4 nm thickness) along the (001) direction. Three dimensional periodic boundary conditions apply. While TiO<sub>2</sub> terminated ((Nd/Pr)O)<sup>+</sup>/(TiO<sub>2</sub>)<sup>0</sup> *n*-type and SrO terminated ((Ga/Al)O<sub>2</sub>)<sup>-</sup>/(SrO)<sup>0</sup> *p*-type IFs are present in our supercells, we will focus in the following only on the *n*-type IFs. Since for polar heterostructures, the electronic states depend critically on structural details at the IF, a structural optimization of the supercells is essential.<sup>28,29</sup> Accordingly, we have fully optimized all heterostructures under consideration by minimizing the forces acting on the atoms. The lattice mismatch for NdGaO<sub>3</sub>, PrAlO<sub>3</sub>, and NdAlO<sub>3</sub> with the SrTiO<sub>3</sub> substrate amounts to 1.6%, 3.1%, and 3.6%, respectively. Since the strain thus is larger in PrAlO<sub>3</sub>/SrTiO<sub>3</sub> and

NdAlO<sub>3</sub>/SrTiO<sub>3</sub> than in NdGaO<sub>3</sub>/SrTiO<sub>3</sub>, a stronger relaxation is found for the former two cases.

Our structural optimization results in a strong buckling in each heterostructure. The IF Ti atoms move along the *c*-direction (out-of-plane), which significantly modifies the bond lengths at and near the IF, see the summarized bond lengths in Table I. The in-plane bond lengths remain almost the same in all the systems. The out-of-plane Ti-O bond lengths increase by 0.05 Å, 0.10 Å, and 0.13 Å, while the out-of-plane A-O bond lengths decrease by 0.03 Å, 0.06 Å, and 0.08 Å for NdGaO<sub>3</sub>/SrTiO<sub>3</sub>, PrAlO<sub>3</sub>/SrTiO<sub>3</sub>, and NdAlO<sub>3</sub>/SrTiO<sub>3</sub>, respectively. In other words, the Ti atoms in the TiO<sub>2</sub> layer and O atoms in the AO layer repel each other, whereas the A atoms and O atoms in the TiO<sub>2</sub> layer attract each other. This situation is similar to the observations for the LaAlO<sub>3</sub>/SrTiO<sub>3</sub> heterostructure.<sup>30</sup> Furthermore, the O-Ti-O bond angles change by 1.5%, 2.8%, and 3.7% and the O-A-O bond angles by 1.0%, 2.1%, and 2.5% in the three heterostructures. Since the TiO<sub>6</sub> octahedra are elongated along the *c*-direction, the threefold degenerate *t<sub>2g</sub>* states of a perfect octahedron split into *d<sub>xy</sub>* and twofold degenerate *d<sub>xz,yz</sub>* manifolds. This reflects a classical Jahn-Teller distortion, which can significantly alter the orbital occupations. We have confirmed the strength of the buckling with an accuracy of 0.01 Å for a non-stoichiometric supercell of NdGaO<sub>3</sub>/SrTiO<sub>3</sub> in which only one type of IF is present.

Figure 2 shows spin polarized Ti 3*d* and O 2*p* DOSs obtained by GGA+*U*+SOC calculations for atoms at (IF layer) and near (IF-1 and IF-2 layers) the *n*-type IFs in NdGaO<sub>3</sub>/SrTiO<sub>3</sub> (left), PrAlO<sub>3</sub>/SrTiO<sub>3</sub> (middle), and NdAlO<sub>3</sub>/SrTiO<sub>3</sub> (right). We observe metallic states for the two (NdO)<sup>+</sup>/(TiO<sub>2</sub>)<sup>0</sup> IFs as well as for the (PrO)<sup>+</sup>/(TiO<sub>2</sub>)<sup>0</sup> IF. The metallicity is mainly due to the Ti 3*d* states with small contributions of the O 2*p* states. Due to charge transfer from the NdO and PrO layers to the TiO<sub>2</sub> layer, the Ti 3*d* states shift considerably to lower energy and become partially occupied. Consequently, the IF Ti atoms develop mixed valency, in

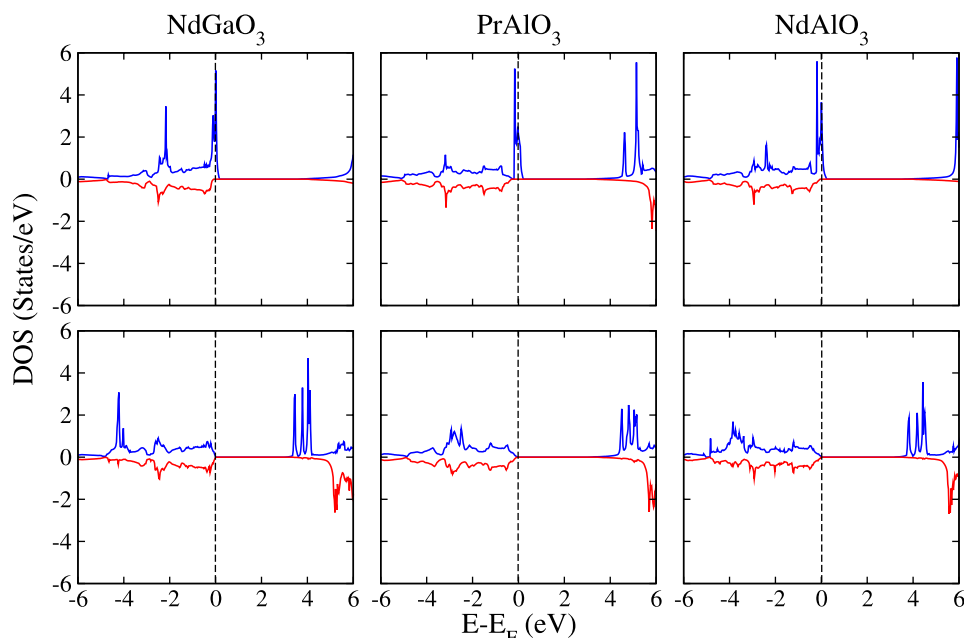


FIG. 1. Total spin polarized DOSs (per unit cell) of bulk NdGaO<sub>3</sub>, PrAlO<sub>3</sub>, and NdAlO<sub>3</sub> obtained by GGA+*U* (top row) and GGA+*U*+SOC (bottom row) calculations with *U* = 7.5 eV for Pr and Nd.

TABLE I. Out-of-plane bond lengths (in Å) and angles (in degrees) at and near the  $n$ -type  $\text{ABO}_3/\text{SrTiO}_3$  ( $A = \text{Nd, Pr}$  and  $B = \text{Ga, Al}$ ) IF.

		Ti-O	Sr-O	O-Ti-O	B-O	A-O	O-A-O
NdGaO <sub>3</sub>	Initial	1.92	2.75	180.0	1.92	2.73	180.0
	Final	1.97	2.79	177.3	1.90	2.70	178.2
PrAlO <sub>3</sub>	Initial	1.89	2.75	180.0	1.89	2.69	180.0
	Final	1.99	2.81	175.1	1.86	2.63	176.3
NdAlO <sub>3</sub>	Initial	1.88	2.75	180.0	1.88	2.68	180.0
	Final	2.01	2.83	173.4	1.82	2.61	175.5

agreement with experiment.<sup>21,22</sup> The Ti  $d_{xy}$  states are lowest in energy and, therefore, mainly responsible for the IF metallicity with a small contribution of the  $d_{xz,yz}$  states. The  $e_g$  orbitals remain unoccupied because they are subject to direct overlap with O  $2p$  orbitals and, therefore, appear at higher energy. The Nd and Pr magnetic moments of atoms at the IF are slightly enhanced to  $3.06 \mu_B$ ,  $3.02 \mu_B$ , and  $2.01 \mu_B$  in NdGaO<sub>3</sub>/SrTiO<sub>3</sub>, NdAlO<sub>3</sub>/SrTiO<sub>3</sub>, and PrAlO<sub>3</sub>/SrTiO<sub>3</sub>, respectively, as compared to the bulk compounds. In order to decide whether this change in the magnetic moments at the IF is a result of the structural relaxation or an electronic effect, we have calculated distorted bulk structures and obtain values of  $3.00 \mu_B$ ,  $2.99 \mu_B$ , and  $1.99 \mu_B$ . Therefore, the modification of the magnetic moments is mainly an electronic effect. For the IF Ti atoms, induced magnetic moments of  $0.08 \mu_B$ ,  $0.04 \mu_B$  and  $0.02 \mu_B$  are found, respectively, while Ti atoms away from the IF carry negligible magnetic moments as the octahedral distortions are much weaker. The elongation of the TiO<sub>6</sub> octahedra due to the lattice mismatch thus determines the induced magnetic moments of the IF Ti atoms. The calculated magnetic moments become smaller with increasing lattice mismatch because the occupation of the Ti  $3d$  orbitals decreases.

For NdGaO<sub>3</sub>/SrTiO<sub>3</sub>, there is experimental evidence from electron energy loss spectroscopy for strong confinement of the free electrons that are responsible for the IF

conductivity within a very narrow region of the SrTiO<sub>3</sub> of about 3 unit cells thickness, which reflects the two dimensional nature of the electron gas.<sup>22</sup> In this region, the Ti  $3d$  states reveal mixed valency between 3+ and 4+ configurations, i.e., they are partially populated and exhibit metallicity. Our calculations nicely confirm this picture. Figure 2 shows that the charge transfer is strongest within the first TiO<sub>2</sub> layer and decreases rapidly away from the IF for all the considered heterostructures. The second TiO<sub>2</sub> layer still contributes to the metallic states, the third TiO<sub>2</sub> layer only little, and all further layers show an insulating nature. Since for NdAlO<sub>3</sub>/SrTiO<sub>3</sub> the 2DEG is confined to only two SrTiO<sub>3</sub> unit cells, it emerges that a large lattice mismatch restricts the charge transfer. To be more specific, the total widths of the metallic regions perpendicular to the IF are found to be  $7.6 \text{ \AA}$ ,  $7.7 \text{ \AA}$ , and  $4.2 \text{ \AA}$  for NdGaO<sub>3</sub>/SrTiO<sub>3</sub>, PrAlO<sub>3</sub>/SrTiO<sub>3</sub>, and NdAlO<sub>3</sub>/SrTiO<sub>3</sub>, respectively. Therefore, the spin polarized 2DEG in these systems is much more confined than in LaAlO<sub>3</sub>/SrTiO<sub>3</sub>, where a thickness of at least 10-20 Å, and thus a still considerable extension in the third dimension are reported.

Analysis of the orbital occupations yields for the Ti  $3d$  states in the IF TiO<sub>2</sub> layer values of 0.07, 0.05, and 0.02 electrons (within the muffin-tin spheres) for NdGaO<sub>3</sub>/SrTiO<sub>3</sub>, PrAlO<sub>3</sub>/SrTiO<sub>3</sub>, and NdAlO<sub>3</sub>/SrTiO<sub>3</sub>, respectively. These occupations correspond to charge carrier densities of  $4.6 \cdot 10^{13} \text{ cm}^{-2}$ ,  $3.1 \cdot 10^{13} \text{ cm}^{-2}$ , and  $1.5 \cdot 10^{13} \text{ cm}^{-2}$ , which are slightly higher than the experimental values at low temperature and pressure.<sup>21,22</sup> The charge carrier density is plotted against the lattice mismatch between the component materials in Fig. 3. A significant interdependence is evident. The larger the lattice mismatch, the smaller is the charge carrier density. This behavior agrees also with the observation for LaAlO<sub>3</sub>/SrTiO<sub>3</sub> that tensile strain destroys the 2DEG.<sup>11</sup> We have tested whether the calculated charge carrier density depends on the value of the onsite interaction on the Ti  $3d$  orbitals. Specifically, we have studied NdGaO<sub>3</sub>/SrTiO<sub>3</sub> for values of  $U = 3 \text{ eV}$  and  $U = 5 \text{ eV}$  and obtain the same charge

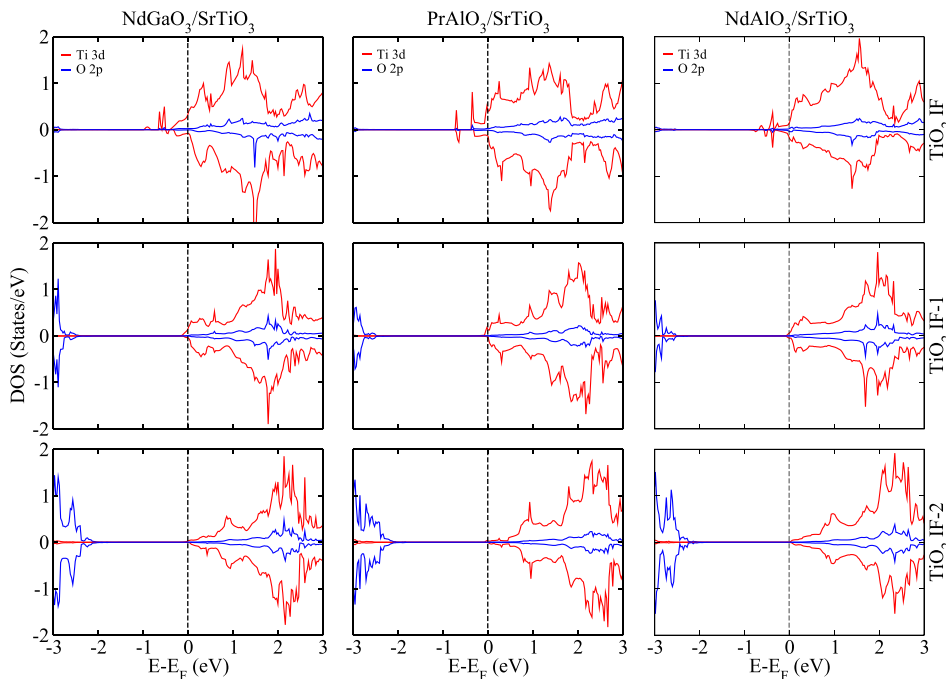


FIG. 2. Spin polarized Ti  $3d$  and O  $2p$  DOSs obtained by GGA+ $U$ +SOC calculations with  $U = 4 \text{ eV}$  and  $7.5 \text{ eV}$  for the Ti  $3d$  and Nd  $4f$  states, respectively.

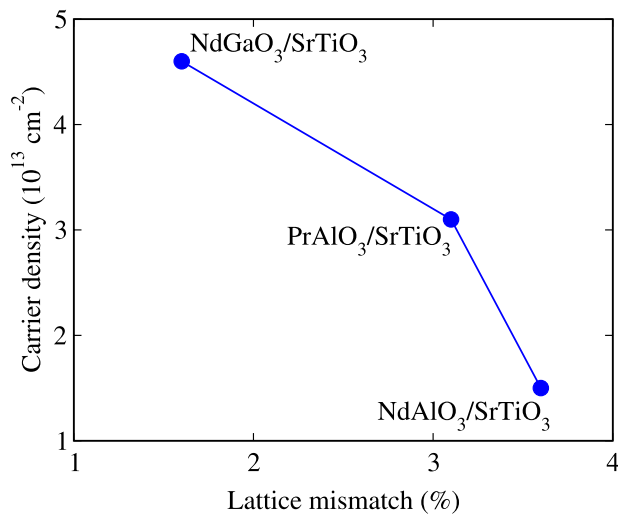


FIG. 3. Charge carrier density of the IF Ti  $3d$  states as function of the lattice mismatch.

carrier density as for  $U = 4 \text{ eV}$  within an accuracy of  $0.1 \cdot 10^{13} \text{ cm}^{-2}$ .

To conclude, the electronic and magnetic properties of the  $n$ -type IFs in the  $\text{ABO}_3/\text{SrTiO}_3$  ( $A = \text{Nd, Pr}$  and  $B = \text{Ga, Al}$ ) heterostructures have been studied by spin polarized density functional theory. Structural optimizations indicate significant modifications of the bond lengths in the  $\text{TiO}_6$  octahedral and, hence, of the chemical bonding. A spin polarized 2DEG is found for each heterostructure. We observe significant charge transfer effects, which decrease rapidly away from the IF. Therefore, the metallic states extend only over a very narrow region of the  $\text{SrTiO}_3$ . It can be expected that the extension of the electron gas decreases further when the thickness of the  $\text{ABO}_3$  layer is reduced. The calculated values of the Ti  $3d$  charge carrier density are higher as compared to the experiment but show the same trend for the different IFs. Importantly, our results demonstrate that an increasing lattice strain due to mismatch between the component materials suppresses the occupation of the spin majority Ti  $3d$  states (hence, the charge carrier density) and, therefore, the spin polarization.

We thank M. Upadhyay Kahaly and B. Amin for valuable discussions and KAUST research computing for providing the computational resources used for this study.

<sup>1</sup>S. Okamoto and A. J. Millis, *Nature* **428**, 630 (2004).

<sup>2</sup>H. W. Jang, D. A. Felker, C. W. Bark, Y. Wang, M. K. Niranjan, C. T. Nelson, Y. Zhang, D. Su, C. M. Folkman, S. H. Baek, S. Lee, K. Janicka, Y. Zhu, X. Q. Pan, D. D. Fong, E. Y. Tsymlal, M. S. Rzchowski, and C. B. Eom, *Science* **331**, 886 (2011).

<sup>3</sup>E. J. Monkman, C. Adamo, J. A. Mundy, D. E. Shai, J. W. Harter, D. Shen, B. Burganov, D. A. Muller, D. G. Schlom, and K. M. Shen, *Nature Mater.* **11**, 855 (2012).

<sup>4</sup>A. Ohtomo and H. Y. Hwang, *Nature (London)* **427**, 423 (2004).

<sup>5</sup>C. Cen, S. Thiel, G. Hammerl, C. W. Schneider, K. E. Andersen, C. S. Hellberg, J. Mannhart, and J. Levy, *Nature Mater.* **7**, 298 (2008).

<sup>6</sup>C. Cen, S. Thiel, J. Mannhart, and J. Levy, *Science* **323**, 1026 (2009).

<sup>7</sup>R. Arras, V. G. Ruiz, W. E. Pickett, and R. Pentcheva, *Phys. Rev. B* **85**, 125404 (2012).

<sup>8</sup>D. A. Dikin, M. Mehta, C. W. Bark, C. M. Folkman, C. B. Eom, and V. Chandrasekhar, *Phys. Rev. Lett.* **107**, 056802 (2011).

<sup>9</sup>M. M. Mehta, D. A. Dikin, C. W. Bark, S. Ryu, C. M. Folkman, C. B. Eom, and V. Chandrasekhar, *Nat. Commun.* **3**, 955 (2012).

<sup>10</sup>B. Kalisky, J. A. Bert, B. B. Klopfer, C. Bell, H. K. Sato, M. Hosoda, Y. Hikita, H. Y. Hwang, and K. A. Moler, *Nat. Commun.* **3**, 922 (2012).

<sup>11</sup>C. W. Bark, D. A. Felker, Y. Wang, Y. Zhang, H. W. Jang, C. M. Folkman, J. W. Park, S. H. Baek, H. Zhou, D. D. Fong, X. Q. Pan, E. Y. Tsymlal, M. S. Rzchowski, and C. B. Eom, *Proc. Natl. Acad. Sci. U.S.A.* **108**, 4720 (2011).

<sup>12</sup>P. Perna, D. Maccariello, M. Radovic, U. Scotti di Uccio, I. Pallecchi, M. Codda, D. Marr, C. Cantoni, J. Gazquez, M. Varela, S. J. Pennycook, and F. M. Granozio, *Appl. Phys. Lett.* **97**, 152111 (2010).

<sup>13</sup>C. Aruta, S. Amoroso, R. Bruzese, X. Wang, D. Maccariello, F. Mileto Granozio, and U. Scotti di Uccio, *Appl. Phys. Lett.* **97**, 252105 (2010).

<sup>14</sup>S. Nazir, N. Singh, and U. Schwingenschlög, *Appl. Phys. Lett.* **98**, 262104 (2011).

<sup>15</sup>C. Aruta, S. Amoroso, G. Ausanio, R. Bruzese, E. di Gennaro, M. Lanzano, F. M. Granozio, M. Riaz, A. Sambri, U. Scotti di Uccio, and X. Wang, *Appl. Phys. Lett.* **101**, 031602 (2012).

<sup>16</sup>M. Takizawa, H. Wadati, K. Tanaka, M. Hashimoto, T. Yoshida, A. Fujimori, A. Chikamatsu, H. Kumigashira, M. Oshima, K. Shibuya, T. Mihara, T. Ohnishi, M. Lippmaa, M. Kawasaki, H. Koinuma, S. Okamoto, and A. J. Millis, *Phys. Rev. Lett.* **97**, 057601 (2006).

<sup>17</sup>S. S. A. Seo, W. S. Choi, H. N. Lee, L. Yu, K. W. Kim, C. Bernhard, and T. W. Noh, *Phys. Rev. Lett.* **99**, 266801 (2007).

<sup>18</sup>J. Biscaras, N. Bergeal, A. Kushwaha, T. Wolf, A. Rastogi, R. C. Budhani, and J. Lesueur, *Nat. Commun.* **1**, 89 (2010).

<sup>19</sup>J. Biscaras, N. Bergeal, S. Hurand, C. Grosssetete, A. Rastogi, R. Budhani, D. LeBoeuf, C. Proust, and J. Lesueur, *Phys. Rev. Lett.* **108**, 247004 (2012).

<sup>20</sup>S. Ueda, N. Kawakami, and M. Sigrist, *Phys. Rev. B* **85**, 235112 (2012).

<sup>21</sup>A. Annadi, A. Putra, Z. Q. Liu, X. Wang, K. Gopinadhan, Z. Huang, S. Dhar, T. Venkatesan, and Ariando, *Phys. Rev. B* **86**, 085450 (2012).

<sup>22</sup>U. Scotti di Uccio, C. Aruta, C. Cantoni, E. D. Gennaro, A. Gadaleta, A. R. Lupini, D. Maccariello, D. Marré, I. Pallecchi, D. Paparo, P. Perna, M. Riaz, and F. M. Granozio, e-print [arXiv:1206.5083](https://arxiv.org/abs/1206.5083).

<sup>23</sup>P. Blaha, K. Schwarz, G. Madsen, D. Kvasnicka, and J. Luitz, *WIEN2K, An Augmented Plane Wave + Local Orbitals Program for Calculating Crystal Properties* (Technical University of Vienna, Vienna, 2001).

<sup>24</sup>M. Djermouni, A. Zaoui, S. Kacimi, and B. Bouhaf, *Comput. Mater. Sci.* **49**, 904 (2010).

<sup>25</sup>G. A. Geguzina and V. P. Sakhnenko, *Crystallogr. Rep.* **49**, 15 (2004).

<sup>26</sup>R. L. Moreira and A. Dias, *J. Phys. Chem. Solids* **68**, 1617 (2007).

<sup>27</sup>A. H. Reshak, M. Piasecki, S. Auluck, I. V. Kityk, R. Khenata, B. Andriyevsky, C. Cobet, N. Esser, A. Majchrowski, O. M. Swirkowicz, R. Diduszko, and W. Szyrski, *J. Phys. Chem. B* **113**, 15237 (2009).

<sup>28</sup>U. Schwingenschlög and C. Schuster, *Chem. Phys. Lett.* **467**, 354 (2009); *EPL* **81**, 17007 (2008).

<sup>29</sup>U. Schwingenschlög and C. Schuster, *EPL* **86**, 27005 (2009).

<sup>30</sup>M. S. Park, S. H. Rhim, and A. J. Freeman, *Phys. Rev. B* **74**, 205416 (2006).